Received: 1 March 2017 | Accepted: 7 April 2017

DOI: 10.1111/jpi.12414

ORIGINAL ARTICLE

WILEY Journal of Pineal Research
Molecular, Biological, Physiological and Clinical Aspects of Melatonin

Melatonin alleviates inflammasome-induced pyroptosis through inhibiting NF-κB/GSDMD signal in mice adipose tissue

Zhenjiang Liu | Lu Gan | Yatao Xu | Dan Luo | Qian Ren | Song Wu | Chao Sun

College of Animal Science and Technology, Northwest A&F University, Yangling, Shaanxi, China

Correspondence
Chao Sun, College of Animal Science and Technology, Northwest A&F University, Yangling, Shaanxi, China.
Email: sunchao2775@163.com

Funding information
National Natural Science Foundation of China, Grant/Award Number: 31572365; Major National Scientific Research Projects, Grant/Award Number: 2015CB943102

Abstract

Pyroptosis is a proinflammatory form of cell death that is associated with pathogenesis of many chronic inflammatory diseases. Melatonin is substantially reported to possess anti-inflammatory properties by inhibiting inflammasome activation. However, the effects of melatonin on inflammasome-induced pyroptosis in adipocytes remain elusive. Here, we demonstrated that melatonin alleviated lipopolysaccharides (LPS)-induced inflammation and NLRP3 inflammasome formation in mice adipose tissue. The NLRP3 inflammasome-mediated pyroptosis was also inhibited by melatonin in adipocytes. Further analysis revealed that gasdermin D (GSDMD), the key executioner of pyroptosis, was the target for melatonin inhibition of adipocyte pyroptosis. Importantly, we determined that nuclear factor κB (NF-κB) signal was required for the GSDMD-mediated pyroptosis in adipocytes. We also confirmed that melatonin alleviated adipocyte pyroptosis by transcriptional suppression of *GSDMD*. Moreover, GSDMD physically interacted with interferon regulatory factor 7 (IRF7) and subsequently formed a complex to promote adipocyte pyroptosis. Melatonin also attenuated NLRP3 inflammasome activation and pyroptosis, which was induced by LPS or obesity. In summary, our results demonstrate that melatonin alleviates inflammasome-induced pyroptosis by blocking NF-κB/GSDMD signal in mice adipose tissue. Our data reveal a novel function of melatonin on adipocyte pyroptosis, suggesting a new potential therapy for melatonin to prevent and treat obesity caused systemic inflammatory response.

KEYWORDS

adipocyte, GSDMD, inflammasome, melatonin, NF-κB, pyroptosis

1 | INTRODUCTION

Obesity has become a public health epidemic worldwide and is associated with adipose tissue inflammation. Dysfunctional adipose tissue with low-grade, chronic, and systemic inflammation links the metabolic and vascular pathogenesis including type II diabetes and cardiovascular disease.[1,2] Studies reveal that hypertrophic adipocytes are immunologically active and capable of activating inflammasome pathways during the chronic inflammation.[3–5] Recent evidences demonstrate that activation of inflammasome pathways triggers pyroptosis and results in the extracellular release of inflammatory cytokines.[6,7] Thus, these findings provide a new potential means for the regulation of inflammasome and pyroptosis in adipocytes to prevent obesity and other chronic inflammatory diseases.

Melatonin (N-acetyl-5-methoxytryptamine) is synthesized by the pineal gland and other organs and maintains

circadian rhythm in mammals.[8–10] Melatonin is involved in a wide range of other physiological functions, including antioxidant, anti-inflammatory, immunomodulatory, and vasomotor effects.[11–14] Our previous study also confirms melatonin promotes proliferation through regulating circadian rhythm in adipocytes.[15] Moreover, studies demonstrate that melatonin ameliorates low-grade inflammation and oxidative stress by repressing the inflammatory response in brain and peripheral tissue.[16–20] Inflammasomes are a group of protein complexes including NLRP3, NLRC4, AIM2, and NLRP6.[21–23] Moreover, inflammasome functions as a sensor to detect danger signals and induce secretion of potent proinflammatory cytokines that contribute to obesity-associated chronic inflammation conditions.[24–26] Recent studies suggest that melatonin attenuates inflammatory response by inhibiting activation of inflammasome in brain and lung injury.[27,28] However, the effects of melatonin on inflammasome of adipocytes during peripheral adipose inflammation remain elusive.

Pyroptosis is an inflammatory form of regulated cell death that relies on cytosolic inflammasome activation.[29] For a long time, pyroptosis has been misclassified as a special type of apoptosis in monocytes in response to certain bacterial insults.[6,30] However, recent studies demonstrate that pyroptosis is emerging as a general innate immune effector mechanism in various cell types.[31,32] Pyroptosis can be triggered by various pathological stimuli, such as microbial infection, stroke, heart attack, or cancer.[30,33] Moreover, Giordano et al.[34] determine that obesity could induce NLRP3-dependent Caspase1 activation and triggers pyroptosis and proinflammatory response in hypertrophic adipocytes. Although several studies reveal the beneficial actions of melatonin on obesity and adipocyte inflammation, the effects of melatonin on pyroptosis in adipocytes are still unknown.

In this study, we investigate the effects of melatonin on inflammasome activation and pyroptosis of adipocytes. We further tested the hypothesis that melatonin could alleviate pyroptosis through the inhibition of NF-κB/GSDMD signals in mice adipose tissues.

2 | MATERIAL AND METHODS

2.1 | Animal experiment

Eight-week-old C57BL/6J background male mice were purchased from the Laboratory Animal Center of the Fourth Military Medical University (Xi'an, China). The use of the animals and mouse handling protocols were conducted following the guidelines and regulations approved by the Animal Ethics Committee of Northwest A&F University (Yangling, Shaanxi). Mice were housed as 2-5 per cage and provided ad libitum with water and a standard laboratory chow diet. The animal room was maintained constant temperature at 25±1°C and humidity at 55±5%, and 12-h light/12-h dark cycles. The mice used for lipopolysaccharide (LPS) challenged and diet-induced obese were maintained in the same condition.

The mice (n=24) were randomly divided into four groups using a 2×2 factorial design. Half of the mice were intraperitoneally injected with phosphate-buffered saline (PBS) (vehicle), and the other half received a daily intraperitoneal (IP) injection of a 200 μL solution consisting melatonin (MT, 20 mg/kg; Sigma-Aldrich, St. Louis, MO, USA) in PBS before the dark onset for 14 days. For the LPS-challenged experiment in vivo, half of the mice that received the PBS or MT injection were challenged via intraperitoneal (ip) injection with the indicated quantities of LPS (75 μg/kg, Sigma-Aldrich, St. Louis, MO, USA) in PBS for 24 hours. Mice were sacrificed by overdosed ethyl ether within two hours after the last injection of melatonin or the vehicle. Immediately, the epididymal white adipose tissue (eWAT) or blood was collected and kept for the studies as follows.

For diet-induced obesity, mice were placed on high-fat diet (HFD; fat provides 60% of the total energy) for 10 weeks, while control mice were fed with a standard chow diet (fat provides 10% of the total energy). Body weight and food intake of mice were recorded weekly. Mice were then euthanized by ethyl ether. The epididymal white adipose tissue (eWAT) was dissected and kept for the following studies.

2.2 | Primary adipocyte culture and reagents treatments

The connective fiber and blood vessels in collected eWAT tissues were removed, and the tissue was washed three times with PBS buffer containing 200 U/mL penicillin (Sigma-Aldrich, St. Louis, MO, USA) and 200 U/mL streptomycin (Sigma, St. Louis, MO, USA). The pre-adipocyte culture was carried out according to our previous publication.[15] Briefly, adipocytes were seeded onto 35-mm culture dishes at 30% (v/v) confluency and incubated at 37°C under a humidified atmosphere of 5% CO_2 and 95% air until confluence. Differentiation of pre-adipocytes was performed as follows. Cells grown to 100% confluence (Day 0) were induced to differentiation using DMEM/F12 medium containing dexamethasone (1 μM, Sigma, St. Louis, MO, USA), insulin (10 μg/mL, Sigma, St. Louis, MO, USA), IBMX (0.5 mM, Sigma, St. Louis, MO, USA) and 10% FBS. Four days after the induction (from Day 2), cells were maintained in the induction medium containing insulin (10 μg/mL, Sigma, St. Louis, MO, USA) and 10% FBS. Melatonin (MT, Selleck.cn, Shanghai, China) was pre-added into culture medium at a final concentration of 1 μM for 14 hours and further stimulated with LPS (200 ng/mL) for another 10 hours. Z-DEVD-FMK (Selleck.cn, Shanghai, China) was added into the culture medium at a final concentration of 50 μM for 24 hours.

For virus vectors study, adipocytes were infected with interference lentiviral recombinant vectors of GSDMD (si-GSDMD), Caspase1 (si-Caspase1), NLRP3 (si-NLRP3), or IRF7 (si-IRF7) for 48 hours at the titer of 1×10^9 IFU/mL and then treated with melatonin. The control vector was pGLVU6-GFP. All the vectors were constructed by Gene Pharma (Shanghai, China).

2.3 | Enzyme-linked immunosorbent assay

The measurement of protein levels of IL-1β, IFN-γ, and IL-6 in cell culture supernatants or mouse sera was taken using the commercial ELISA kits from Sigma (Sigma-Aldrich, St. Louis, MO, USA) according to the manufacturer's instructions.

2.4 | RNA-seq analysis

Total RNA from epididymal adipose tissue (eWAT) was prepared with TRIpure Reagent kit (Takara, Dalian, China) and the RNA-seq analysis was performed as previous described.[15] Briefly, quantification and quality control of the sample libraries were assessed by Agilent 2100 Bioanalyzer and ABI StepOnePlus Real-time PCR System. RNA sequencing was performed using Hiseq 4000 instrument (Illumina, San Diego, CA, USA). Real-time analysis was used for base calling. Fastq files were mapped to the mouse genome (NCBI37/mm9) using TopHat (version 2.0.4, Johns Hopkins University, Baltimore, MD, USA). Mapped reads were then assembled via Cufflinks (version 2.0.2, University of Washington Seattle, WA, USA) with the default settings. Assembled transcripts were then merged using the Cuffmerge program with the reference genome. Analysis of mRNA levels was carried out using the Cuffdiff program, with samples being grouped by treatment condition, three replicates per group. Volcano plots comparing log10 (statistical relevance) to log2 (fold change) were generated using R (version3.1.1, AT&T Bell Laboratories, New York, NY, USA), using the base plotting system and calibrate library. Gene Ontology (GO) and pathway enrichment analysis were performed to categorize the considerably enriched functional classification or metabolic pathways in which DEGs operated.

2.5 | Measurement of Caspase1 and Caspase3 activity

Caspase1 and Caspase3 activities were determined using a Caspase-Glo® 3 Assay Systems (Promega, Madison, WI, USA) and Caspase-Glo® 1 Inflammasome Assay (Promega, Madison, WI, USA) according to the manufacturer's instructions. In brief, cells were seeded in 96-well plate. After treatment, equal volume of Caspase-Glo 3 or 1 reagent was added to the cell culture medium, which had been equilibrated to room temperature for 1 hour, cells were shook for 5 minutes and incubated at room temperature for 30 minutes. Luminescent recording was performed with Victor X (PerkinElmer, MA, USA).

2.6 | Cytotoxicity assay

Relevant adipocytes were treated as indicated. Cytotoxicity was determined by measuring the release of lactate dehydrogenase (LDH) using the CytoTox 96 Non-Radioactive Cytotoxicity Assay kit (Promega, Madison, WI, USA) following the manufacturer's instructions.

2.7 | Immunofluorescence assay

Immunofluorescence analysis was performed as previously described.[35] The cells were treated as indicated and followed fixed with 4% paraformaldehyde and then blocked with 5% bovine serum albumin (BSA) in PBS for 1 hour at room temperature. The cells were then incubated with rabbit polyclonal anti-ASC primary antibody (Abcam, Cambridge, UK) and anti-P65 antibody (Abcam, Cambridge, UK) at a dilution of 1:50 overnight, followed by incubation with fluorescein isothiocyanate-conjugated goat anti-rabbit IgG antibody (Boster, Wuhan, China) for 1 hour at room temperature. DAPI was used for nuclear staining. Finally, cells were observed and photographed using a Cytation3 Cell Imaging Multi-Mode Reader (BioTek, Winooski, VT, USA).

2.8 | Cell death analysis

Adipocytes were incubated for 30 minutes with Hoechst 33342 (Solarbio, Beijing, China) loading dye and washed three times with ice-cold PBS. Mid-stage and late-stage apoptosis of adipocytes were assayed using Annexin V-FITC/PI apoptosis detection kit (Beyotime Institute of Biotechnology, Nanjing, China) following the User Protocol. Terminal deoxynucleotidyl transferased UTP nick-end labeling (TUNEL) staining was further used to detect apoptosis using the commercial kit from Vazyme (TUNEL BrightGreen Apoptosis Detection Kit, Vazyme, Nanjing, China). The TUNEL-positive cells showed green nuclear staining, and all of the cells with blue nuclear DAPI staining were counted within five randomly chosen fields under high power magnification. The index of apoptosis was expressed as the ratio of positively stained apoptotic cells to the total number of cells counted ×100%. The cells were visualized and analyzed using Cytation3 Cell Imaging Multi-Mode Reader (BioTek, Winooski, VT, USA) and using BD FACScan (BD Biosciences, Franklin Lakes, NJ, USA). Data were analyzed using Cell Quest software (BD Biosciences).

2.9 | Transmission electron microscopy

At room temperature, adipocytes were fixed in 2.5% glutaraldehyde in PBS (pH=7.2) for 24 hours, postfixed in 1% osmium tetroxide in water for 2 hours. After dehydrated in an ascending series of ethanol (30%, 50%, 70%, 80%, 90%, 100%) for 10 minutes each, the samples were then embedded in Durcupan ACM (Fluka Chemie AG, Buchs, Switzerland). Sections were cut with a diamond knife at a thickness of 50-60 nm. These sections were stained with uranyl acetate and lead citrate and examined with a transmission electron microscopy (TEM, HT7700, 80 kV, Hitachi, Tokyo, Japan). Images were recorded on film at 30 000×magnification. The percentage of mitochondrial integrity was determined by dividing the number of normal mitochondria by the total number of mitochondria per image.

2.10 | Plasmids construction and Dual-luciferase reporter assay

A 850-bp mouse *GSDMD* promoter was cloned by PCR amplification of C57BL/6J mouse genomic DNA and inserted in the pGL-3 basic vector (Promega, Madison, WI, USA). The resulting reporter was named $GSDMD_{850}$-Luc. Further deletion of the $GSDMD_{850}$-Luc generated $GSDMD_{720}$-Luc, $GSDMD_{250}$-Luc, and $GSDMD_{100}$-Luc reporters contained of 720 bp, 250 bp and 100 bp of *GSDMD* promoter, respectively. Mutant GSDMD reporter plasmids were generated using the $GSDMD_{720}$-Luc plasmid as a template; a mutagenesis kit (Invitrogen, CA, USA) was used to created $GSDMD_{720}$-Luc-S1, $GSDMD_{720}$-Luc-S2 and $GSDMD_{720}$-Luc-S1, S2 with mutation in the two binding sites of *GSDMD* promoter. HEK293 cells were cotransfected with luciferase reporter plasmids, pRL-TK reporter plasmid (control reporter), and NF-κB plasmid (pc-NF-κB) using X-tremeGENE™ Transfection Reagent (Roche, Basel, Switzerland). After transfection for 24 hours, cells were harvested and measured using the Dual-Luciferase Reporter assay system (Promega, Madison, WI, USA), and luciferase activity was divided by the Renilla luciferase activity to normalize for transfection efficiency.

2.11 | Chromatin Immunoprecipitation (ChIP) assay

ChIP assay was performed as previous described using a ChIP assay kit (Abcam, Cambridge, UK) according to the manufacturer's protocol. In brief, primary antibodies of GSDMD (Abcam, Cambridge, UK) or IgG (Abcam, Cambridge, UK) were used. DNA–protein cross-linking complexes were collected, and purified DNA was subjected to qPCR with SYBR green fluorescent dye (Invitrogen, Carlsbad, CA, USA).

2.12 | Nuclear protein extraction

Nuclear and cytoplasmic fractions were prepared using the protocols from Zhong et al.[36] In brief, cells were lysed with 400 μL of cytoplasmic lysis buffer. The lysates were incubated for 5 minutes on ice and vortexed two times for 10 seconds. The lysates were centrifuged for 30 seconds at 16 000×*g*, and supernatants were collected as cytoplasmic fractions. The pellets were resuspended in 50 μL of nuclear extraction buffer and sonicated three times on ice. The nuclear fractions were centrifuged for 5 minutes at 16 000×*g*, and the supernatant was collected to obtain nuclear proteins. The proteins were denatured by boiling at 100°C and kept for further studies.

2.13 | Co-immunoprecipitation (Co-IP) analysis

HEK293 cells were transfected with plasmids using X-tremeGENE™ Transfection Reagent (Roche, Basel, Switzerland). After 24-h transfection, cells were then snap-frozen in lipid nitrogen. Whole-cell lysate was harvested in lysis buffer with a protease inhibitor. Cells were then sonicated for 10 seconds, and the whole-cell lysate was pre-cleared with Protein A for 2 hours and incubated with 2 μg primary antibody overnight at 4°C. Immune complexes were pulled down with Protein A agarose for 2 hours at 4°C with shaking. Beads were washed once with lysis buffer and three times with wash buffer and then eluted by boiling in SDS sample buffer followed by detection of Western blot.

2.14 | Real-time quantitative PCR analysis

Total RNA was extracted from eWAT or adipocytes with TRIpure Reagent kit (Takara, Dalian, China) as previously described;[37] 500 ng of total RNA was reverse-transcribed using M-MLV reverse transcriptase kit (Takara, Dalian, China). Primers were synthesized by Invitrogen (Shanghai, China). Quantitative PCR was performed in 25 μL reaction system containing specific primers and AceQ qPCR SYBR Green Master Mix (Vazyme, Nanjing, China). Amplification was performed in the ABI StepOne Plus™ RT-PCR System (ABI, Carlsbad, CA). The levels of mRNA were normalized in relevance to GAPDH. The expression of genes was analyzed by method of $2^{-\Delta\Delta C_t}$.

2.15 | Western blotting analysis

Protein from adipocytes was extracted using lysing buffer according to the protocol from Liu et al.[38] Protein concentration was determined using BCA Protein Assay kit (Beyotime Institute of Biotechnology, Nanjing, China). Proteins (30 μg) were separated by SDS-PAGE, transferred to PVDF

nitrocellulose membrane (Millipore, Boston, MA, USA), blocked with 5% fat-free milk for 2 hours at room temperature, and then incubated with primary antibodies in 5% milk overnight at 4°C. p65, phosphorylate-p65, NLRP3, GSDMD, ASC, Caspase1, Cleaved-Caspase1, Caspase3, Cleaved-Caspase3, NF-κB, phosphorylate-NF-κB, and IRF7 antibodies were all purchased from Abcam (Cambridge, UK), and GAPDH from Bioworld (Nanjing, China). Rabbit HRP-conjugated secondary antibody (Baoshen, Beijing, China) was added and incubated at room temperature for 2 hours. Proteins were visualized using chemiluminescent peroxidase substrate (Millipore, Boston, MA, USA), and then the blots were quantified using ChemiDoc XRS system (Bio-Rad, Hercules, CA, USA).

2.16 | Statistical analysis

Statistical analyses were conducted using SAS v8.0 (SAS Institute, Cary, NC). Data were analyzed using one-way and two-way ANOVAs. Comparisons among individual means were made by Fisher's least significant difference (LSD). Data were presented as mean±SEM. $P<.05$ was considered to be significant.

3 | RESULTS

3.1 | Melatonin reduces inflammasome activation in white adipose tissue

To explore the effects of melatonin on inflammation, we compared white adipose transcriptomes from vehicle- and melatonin-injected mice. Melatonin treatment resulted in an anti-inflammatory transcriptional signature defined by the downregulation of 3, 199 genes when significant gene expression differences are grouped and visualized as a Heatmap (Figure 1A). And further analyses revealed signature genes downregulated by melatonin were associated with inflammasome activation; especially, *NLRP1*, *NLRP3*, and *ASC* were significantly reduced (Figure 1A). The subsequent Gene Ontology (GO) analysis showed the distinct difference genes were enriched in those encoding factors involved in NF-κB signal, NLR signal, and IL signal (Figure 1B). The mRNA expression measurement established that inflammasome indicators *NLRP3* and *ASC* were decreased with melatonin injection. In addition, the levels of *Caspase1* and *IL-1*β, the up- and downstream markers of inflammasome, were all reduced (Figure 1C). Interestingly, melatonin injection significantly decreased the expression of *GSDMD* and *IRF7* (Figure 1C). And the Western blot measurement showed the consistent results (Fig. S1A). The genes described in Figure 1C were virtually all shown by the RNA-sequencing (RNA-Seq) analysis in Figure 1A. Additionally, melatonin injection significantly reduced the serum levels of IL-1β, IL-6, and IFN-γ (Figure 1D-F). These findings indicated melatonin affects the inflammasome activation of white adipose tissue.

3.2 | Melatonin blunts LPS-induced NLRP3 inflammasome activation in adipocytes

To further analyze the regulation of melatonin on inflammasome activation, we pretreated adipocytes with LPS and examined the key inflammasome activity. As expected, LPS treatment stimulated the upregulation of *NLRP3*, *ASC*, and *Caspase1* and also increased the mRNA level of *GSDMD* (Figure 2A). On the contrary, cells treated with melatonin showed the opposite results (Figure 2A). Melatonin can also effectively block LPS-induced IL-1β release (Figure 2B). We next asked whether melatonin affected ASC on protein level. Immunofluorescence stain indicated that ASC protein level was elevated with LPS treatment and decreased when incubated with melatonin (Figure 2C). In addition, melatonin markedly inhibited LPS-induced LDH release, and along with the reduction in Caspase1 and Caspase3 protein contents, indicating the negative role of melatonin on cell death (Figure 2D-F).

3.3 | Melatonin alleviates LPS-induced pyroptosis in adipocytes

To find the distinct role of melatonin in the regulation of cell death, we first used Z-DEVD-FMK, the specific inhibitor of Caspase3, to block cell apoptosis. Figure 3A shows Caspase3 was effectively inhibited in cells pretreated with LPS and Z-DEVD-FMK, and melatonin further reduced the protein level of Caspase3. Z-DEVD-FMK had no effect on Caspase1 (Figure 3B). In addition, melatonin can still reduce LPS-induced Caspase1 elevation with Z-DEVD-FMK treatment (Figure 3B). Similarly, melatonin decreased LPS-induced LDH release and the addition of Z-DEVD-FMK did not disturb this process (Figure 3C). We also performed the TUNEL stain measurement to see how melatonin affected cell death. Interestingly, we obtained the consistent result as in Figure 3A-C; melatonin significantly reduced LPS-induced cell death, while Caspase3 played no role in LPS-mediated cell death (Figure 3D). These results triggered us to hypothesize that melatonin attenuated LPS-induced pyroptosis but not apoptosis in adipocytes. We further examined the NLRP3 and ASC inflammasome and the expression level of *GSDMD*. As expected, melatonin markedly downregulated the mRNA levels of *NLRP3*, *ASC*, and *GSDMD*; and when inhibited Caspase3 activity, melatonin still reduced the levels of inflammasome and *GSDMD* (Figure 3E). IL-1β maturation and secretion is another major response of canonical inflammasome activation. We observed that contrast to control group, melatonin treatment group had little IL-1β

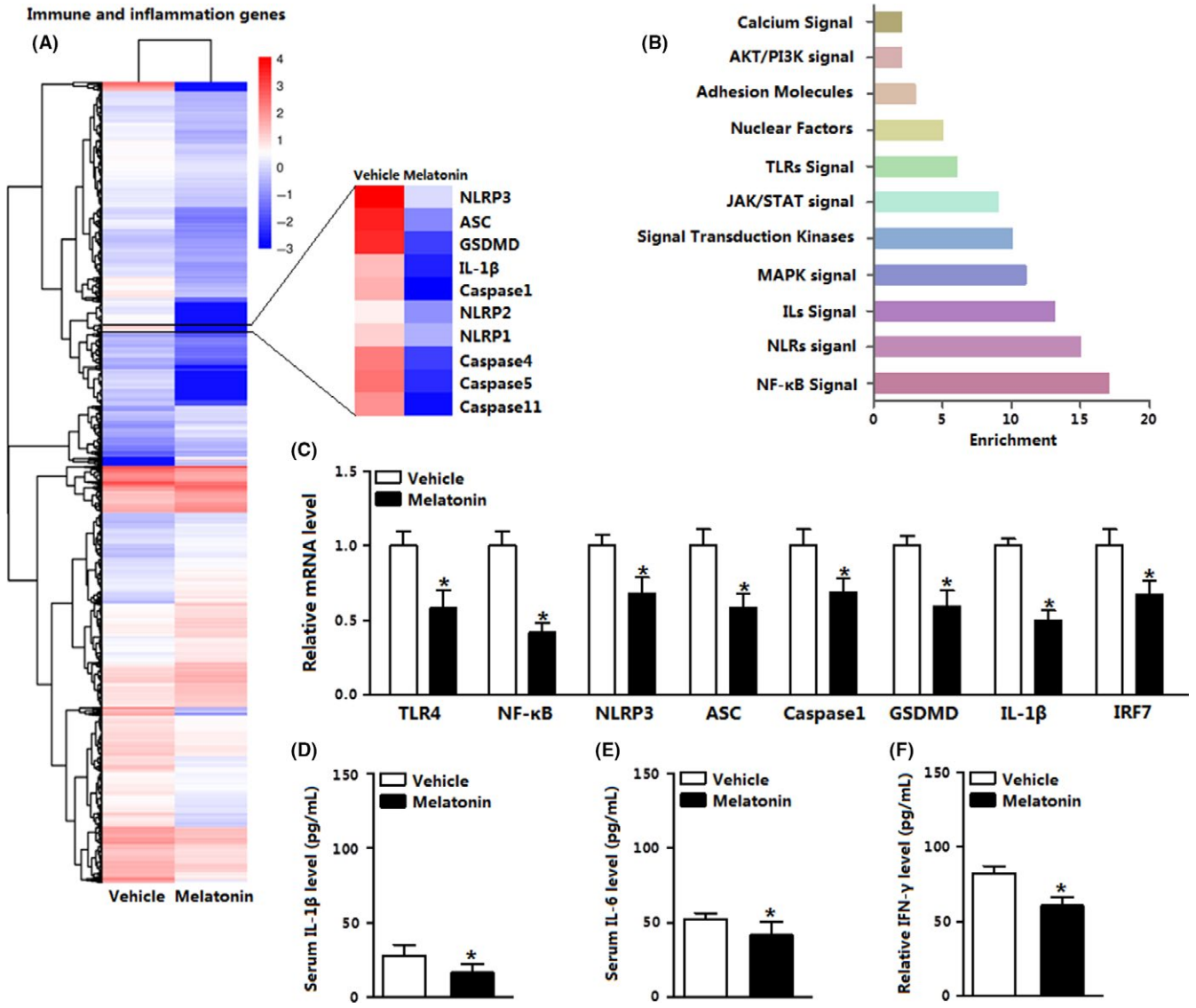

FIGURE 1 Melatonin reduces inflammasome activation in white adipose tissue. A, Heatmap of genes upregulated or downregulated with melatonin injection of mice white adipose tissue, along with the top affected genes with melatonin treatment (n=3). B, GO analysis of the target genes in (A) showing the biology process for melatonin treatment (n=3). C, mRNA levels of inflammation marker genes and inflammasome genes with melatonin treatment of mice white adipose tissue (n=6). D, Serum IL-1β level with melatonin treatment (n=6). E, Serum IL-6 level with melatonin treatment (n=6). F, Serum IFN-γ level with melatonin treatment (n=6). Values are means±SEM. **P*<.05 compared with the control group

secretion into the supernatant, and the inhibition of Caspase3 had no effects on IL-1β secretion (Figure 3F). Thus, we conclude melatonin alleviates LPS-induced pyroptosis.

3.4 | Reduction in GSDMD is essential for melatonin-alleviated pyroptosis

We further examine the regulation of melatonin in inflammasome-triggered pyroptosis. Melatonin decreased the mRNA level of *GSDMD*, and the deficiency of *GSDMD* further strengthens the reduction in *GSDMD* (Figure 4A). Knockdown of GSDMD blocked LPS-induced pyroptosis of adipocytes upon the reduction in *NLRP3* inflammasome and *Caspase1* expression (Figure 4B). Melatonin addition further decreased pyroptosis (Figure 4B). LPS-induced IL-1β release was also inhibited after GSDMD knocked down, and melatonin strengthens the reduction in IL-1β release (Figure 4C). The LPS-induced LDH release was significantly reduced in the si-GSDMD group and melatonin-treated group (Figure 4D). Cotreatment of si-GSDMD and melatonin slightly affected the reduced pattern of LDH (Figure 4D). Compared with LPS treatment group, the deficiency of GSDMD reduced membrane pore formation, suggesting the reduction in pyroptosis (Figure 4E). We got the similar results in melatonin treatment group, and LPS-triggered pyroptosis was further decreased in si-GSDMD and melatonin

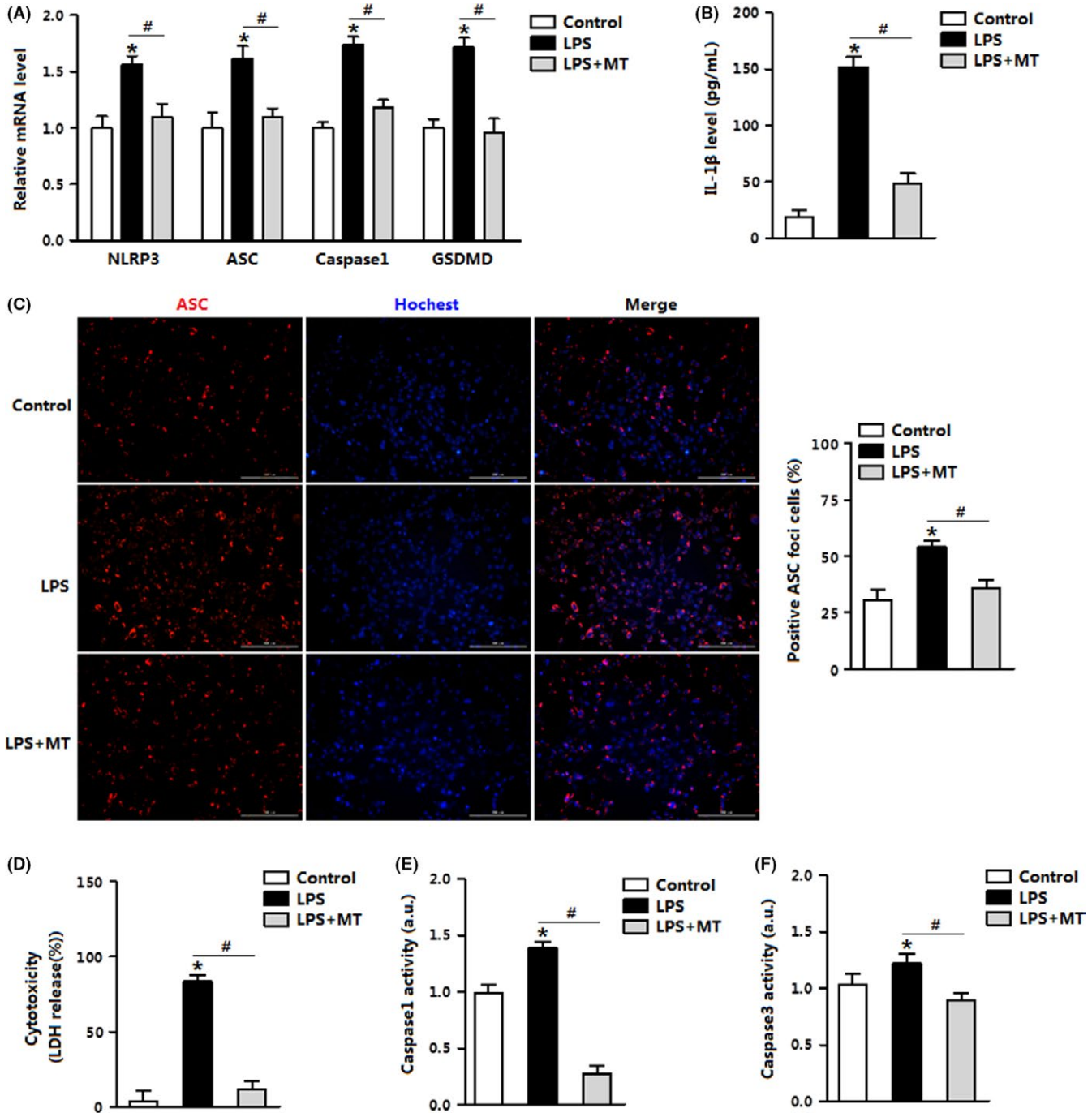

FIGURE 2 Melatonin blunts LPS-induced NLRP3 inflammasome activation in adipocytes. Melatonin was pre-added into culture medium at a final concentration of 1 μM for 14 h and further stimulated with LPS (200 ng/mL) for 10 h. A, Expression profile of *NLRP3*, *ASC*, *Caspase1*, and *GSDMD* of treated adipocytes (n=3). B, IL-1β release in the culture medium was measured by ELISA (n=3). C, Immunofluorescence of ASC and Hoechst staining of treated adipocytes (n=3). D, LDH release was measured in treated adipocytes (n=3). E, Caspase1 activity was detected in treated adipocytes (n=3). F, Caspase3 activity was detected in treated adipocytes (n=3). Values are means±SEM. **P*<.05 compared with the control group, $^{\#}P$<.05 compared with the LPS group

cotreatment group (Figure 4E). We then pretreated cells with Z-DEVD-FMK and performed the TUNEL stain measurement, which confirmed that melatonin attenuated pyroptosis through the regulation of GSDMD (Figure 4F). Together, we confirmed that melatonin alleviated LPS-induced pyroptosis, and the deficiency of GSDMD promoted the this function.

3.5 | Melatonin inhibits adipocyte pyroptosis by reducing NF-κB signal

As indicated in Figure 1, NF-κB signals were enriched in the GO signal pathway analysis, we then asked whether NF-κB signals influenced melatonin function. Firstly, with the

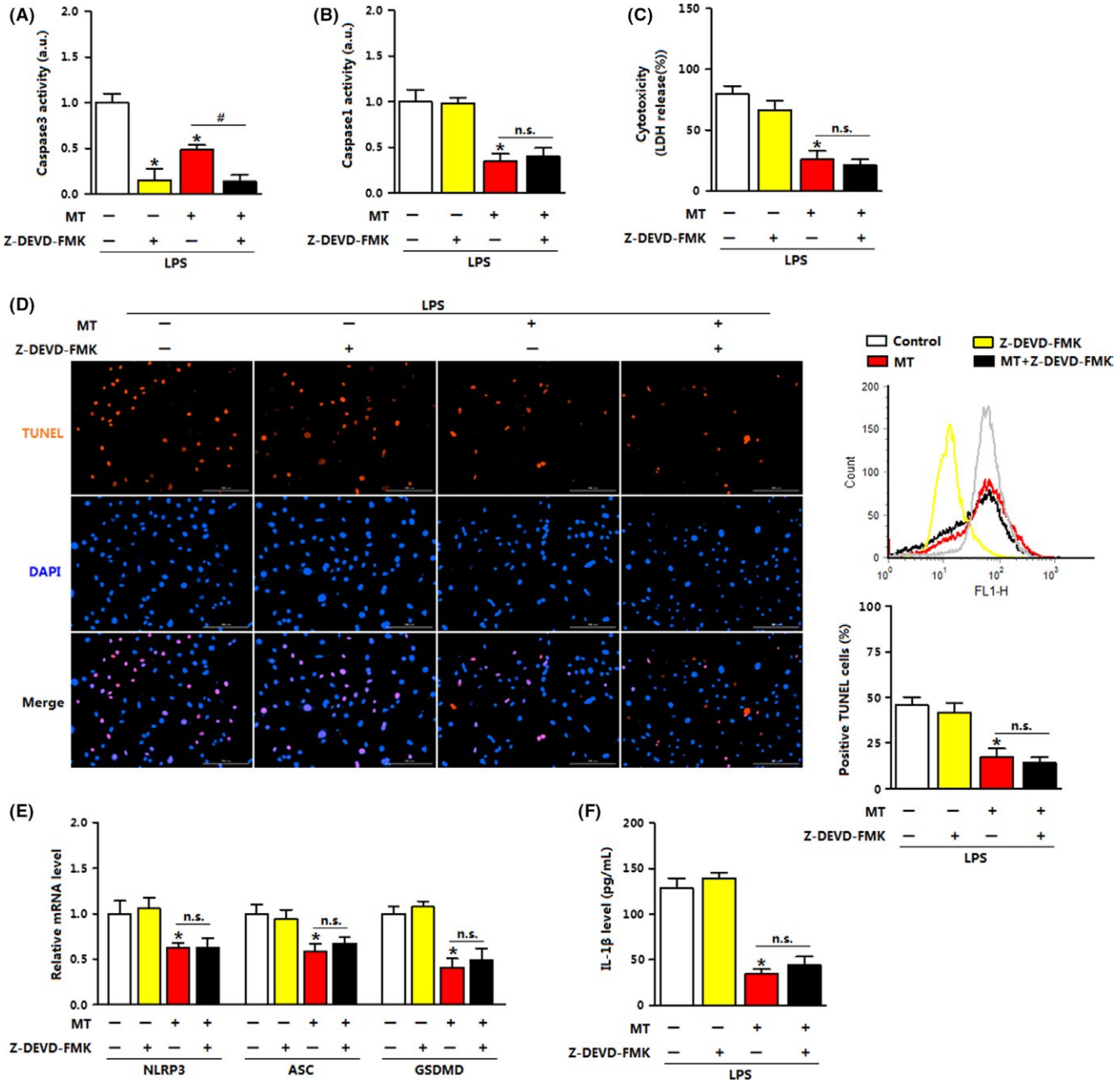

FIGURE 3 Melatonin alleviates LPS-induced pyroptosis in adipocytes. Cells were stimulated with LPS for 24 h and treated with melatonin or Z-DEVD-FMK. A, Caspase3 activity was measured in treated adipocytes (n=3). B, Caspase1 activity was measured in treated adipocytes (n=3). C, LDH release was measured in treated adipocytes (n=3). D, TUNEL staining of treated adipocytes and flow cytometry analysis of positive TUNEL cells (n=3). E, Expression profile of *NLRP3*, *ASC*, and *GSDMD* in treated adipocytes (n=3). F, IL-1β production in culture medium measured by ELISA (n=3). Values are means±SEM. **P*<.05 compared with the control group, $^{\#}P$<.05 compared with the MT group

stimulation of LPS we determined the mRNA and protein levels of melatonin receptors after incubation with melatonin. Figure 5A,B shows both MT1 and MT2 were elevated with melatonin treatment, while LPS had the opposite effects (Figure 5A,B). Melatonin-alone treatment significantly blocked NF-κB signal activity, both the protein level of NF-κB in the cytoplasm and p65 in the nucleus (Figure 5C). And in the cells of LPS-induced pyroptosis, melatonin still reduced the levels of NF-κB and p65 (Figure 5C). Melatonin treatment decreased the *GSDMD* mRNA level, which was elevated by LPS (Figure 5D). In addition, phosphorylation level of p65 was also decreased compared with that in LPS-alone treatment group (Figure 5E). Consistently, the translocation of NF-κB to the nucleus in adipocytes was analyzed using immunofluorescence staining, and the images revealed that NF-κB p65 was normally sequestered in cytoplasm and that both cytoplasm and nuclear accumulation of p65 were markedly reduced following melatonin treatment (Figure 5F).

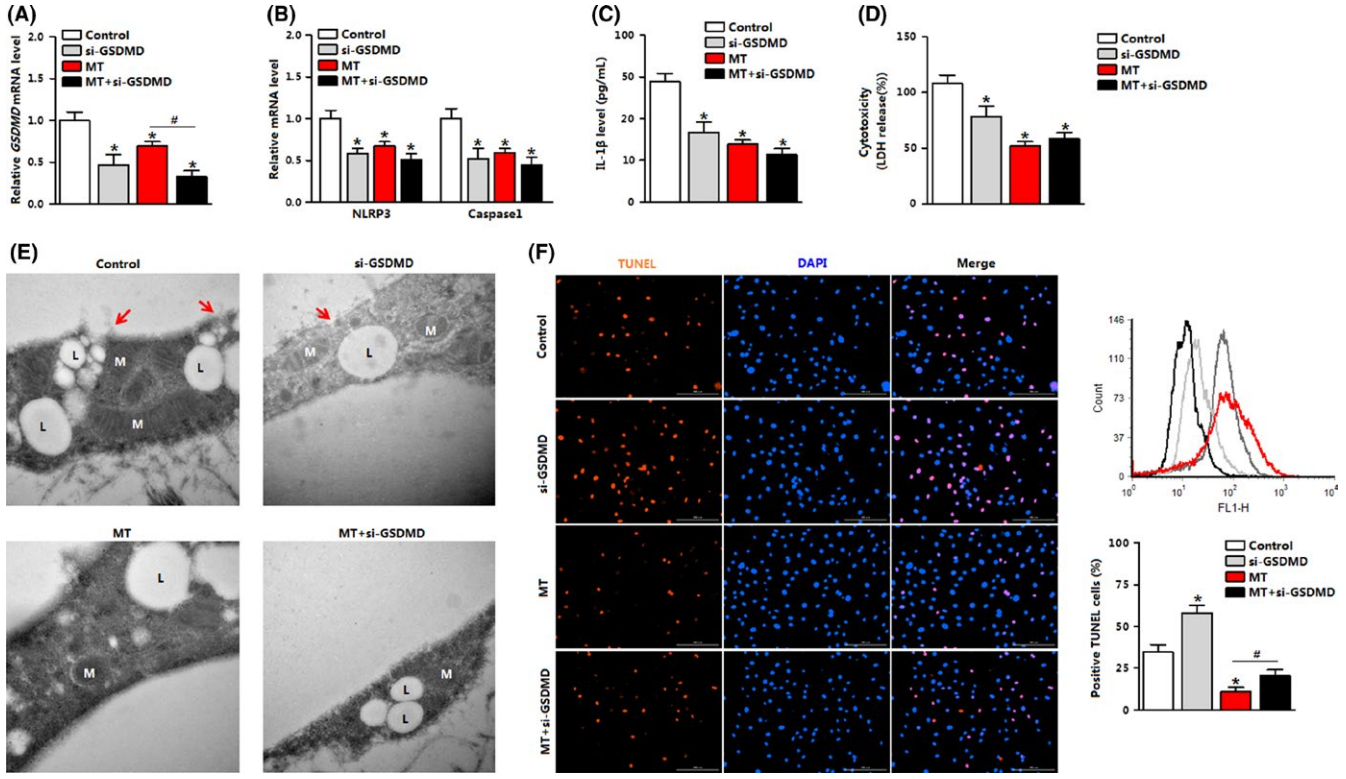

FIGURE 4 Reduction in GSDMD is essential for melatonin-alleviated pyroptosis. Adipocytes were pre-infected with si-GSDMD and then treated with or without melatonin (MT). A, mRNA level of *GSDMD* in treated adipocytes (n=3). B, Gene expression of *NLRP3* and *Caspase1* in treated adipocytes (n=3). C, IL-1β release in the culture medium was measured by ELISA (n=3). D, LDH release was measured in treated adipocytes (n=3). E, Representative electron micrographs (30 000×) of treated adipocytes. Red arrowhead: membrane pores, L: lipid, M: mitochondria (n=3). F, TUNEL staining of treated adipocytes and flow cytometry analysis of positive TUNEL cells (n=3). si-GSDMD: the interference lentivirus vector of GSDMD. Values are means±SEM. **P*<.05 compared with the control group, $^{\#}P$<.05 compared with the MT group

LPS-induced pyroptosis upregulated the protein levels of GSDMD and ASC, and melatonin played the opposite role (Figure 5G). LPS-induced pyroptosis increased the phosphorylation of NF-κB, and along with the elevation of NLRP3 and Cleaved-Caspase1; and melatonin treatment reversed the expression pattern of these indicators (Figure 5G). Interestingly, our data showed LPS-induced pyroptosis enhanced the level of IRF7, which we did not consider before (Figure 5G).

Cluster of transcription factors of multiple inflammation genes were altered as shown in the RNA-seq data (Figure 1). To analyze the underlying mechanisms of melatonin on pyroptosis, we considered the transcription-level control. Our results showed GSDMD promoter contained three potential binding domains of NF-κB (Figure 6A), and data demonstrated the binding sites, 720 bp-250 bp and 250 bp-100 bp upstream of the initiation site of GSDMD, functioned (Figure 6A,B). Mutation of either one of the two binding sites plays no role in the inhibition of GSDMD transcription, but in case of mutant two of the binding sites, the transcription of GSDMD was blocked (Figure 6C). This confirmed both the two binding sites functioned and NF-κB was a positive transcription regulator of GSDMD. Expression of *NF-κB* in adipocytes also increased the expression of *GSDMD*, while cotreatment of NF-κB and melatonin blocked the elevation of *GSDMD* (Figure 6D). Compared with the increasing LDH release and IL-1β release in NF-κB forced expression group, melatonin plus NF-κB reduced both the LDH release and IL-1β release (Figure 6E).

3.6 | IRF7 forms a complex with GSDMD

The decreased protein level of IRF7 caused by melatonin led us to further hypothesize that melatonin regulated LPS-induced pyroptosis by direct modification, through a physical interaction. Based on the bioinformatics analysis and previous data sheet, our data showed IRF7 interacted with GSDMD (Figure 7A). Then by protein–protein measurement, our data indicated IRF7 strongly interacted with GSDMD in HEK293T cells (Figure 7B).

Next, we infected adipocytes with pAd-IRF7 (or si-IRF7) alone or with melatonin and analysis the level of *Caspase1* and IL-1β release. IRF7 overexpression significantly increased *Caspase1* mRNA level, but melatonin addition attenuated the elevation of *Caspase1* (Figure 7C). Similarly, IRF7 stimulated IL-1β release, but melatonin played on the contrary (Figure 7D). Thus, these data

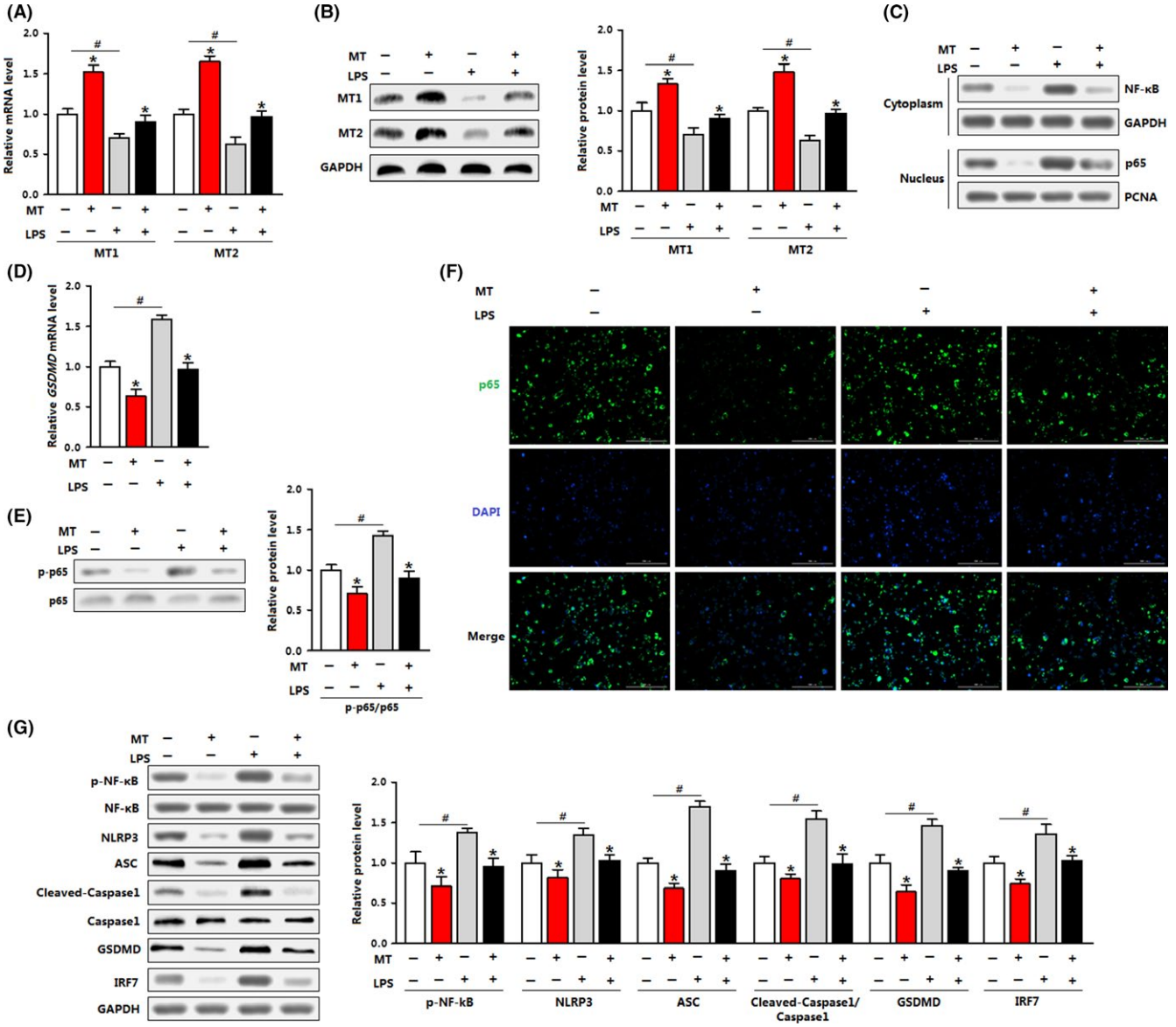

FIGURE 5 Melatonin inhibits adipocyte pyroptosis by reducing NF-κB signal. Adipocytes were pretreated with LPS and incubated with or without melatonin (MT). A, Expression profile of melatonin receptor 1 (*MT1*) and melatonin receptor 2 (*MT2*) in treated adipocytes (n=3). B, Protein levels of melatonin receptor 1 (MT1) and melatonin receptor 2 (MT2) in treated adipocytes (n=3). C, Protein levels of NF-κB and p65 in the cytoplasm and in the nucleus of treated adipocytes (n=3). D, mRNA level of GSDMD in treated adipocytes (n=3). E, Protein level of phosphorylation of p65 and total p65 in treated adipocytes (n=3). F, p65 protein localization was determined using an anti-p65 antibody and fluorescein isothiocyanate-labeled anti-rabbit IgG antibody in treated adipocytes (n=3). G, Protein levels of phosphorylation of NF-κB, total NF-κB, NLRP3, ASC, Cleaved-Caspase1, Caspase1, GSDMD, and IRF7 in treated adipocytes (n=3). Values are means±SEM. **P*<.05, #*P*<.05 compared with the control group

suggested IRF7 and GSDMD directly bind, and melatonin regulated GSDMD-mediated pyroptosis via the regulation of IRF7 in adipocytes.

3.7 | Melatonin alleviates LPS-induced pyroptosis in mice adipose tissue

To test the effects of melatonin on pyroptosis in vivo, we used a model of LPS-induced pyroptosis. LPS treatment markedly increased serum IL-1β level, and melatonin injection had the opposite effect as the in vitro experiments (Figure 8A). Then, further inflammasome detection demonstrated melatonin downregulated LPS-induced *NLRP3* and *ASC* elevation, and along with the reduction in *Caspase1* and GSDMD (Figure 8B). GSDMD membrane pore was also reduced after melatonin treatment in LPS-induced pyroptosis (Figure 8C). Thus, we verified melatonin function in LPS-induced pyroptosis in vivo.

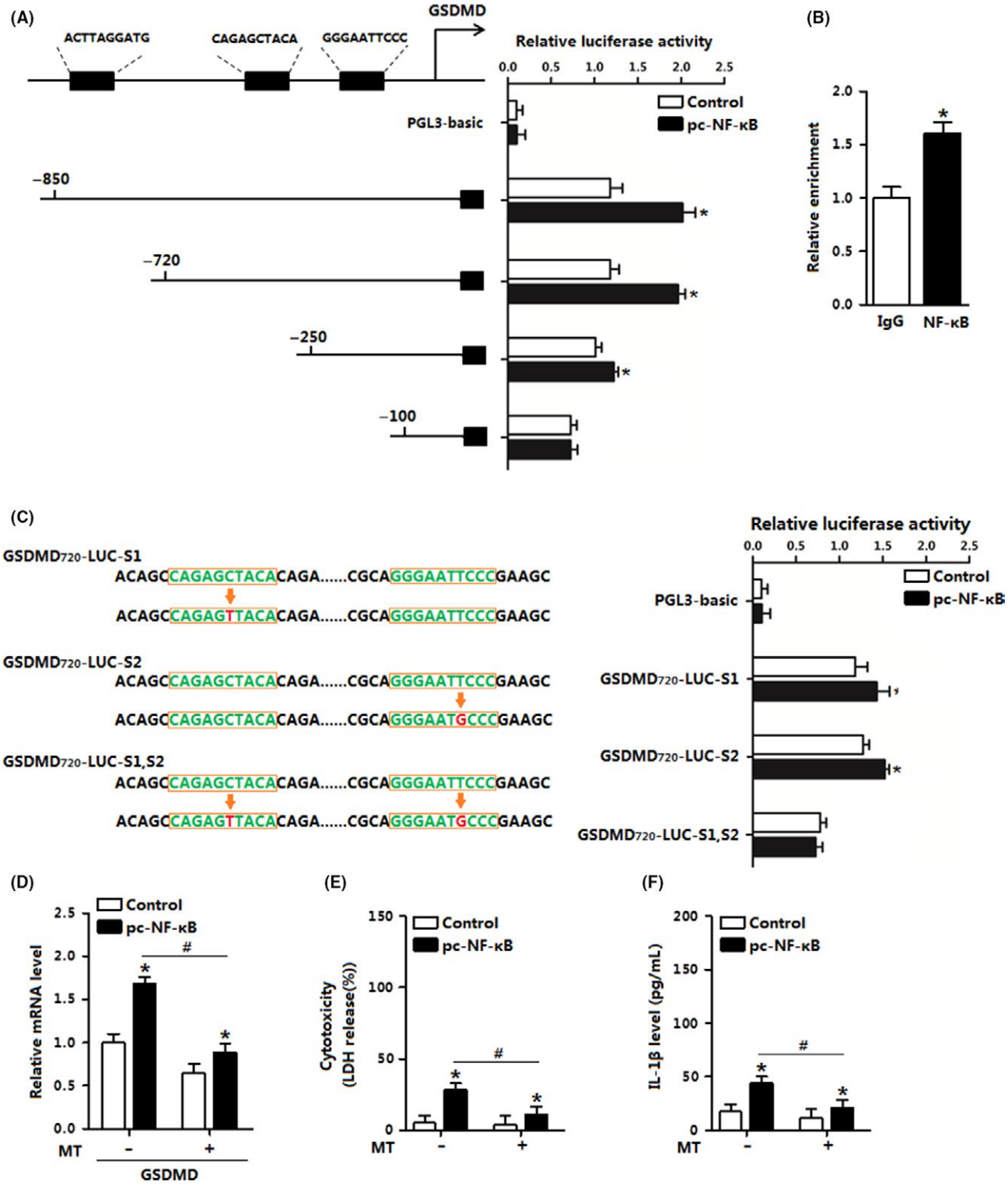

FIGURE 6 NF-κB positively regulated the transcription of GSDMD. A, Dual-luciferase reporter assay of GSDMD and NF-κB. HEK293 cells were transfected with PGL3-basic or PGL3-GSDMD plasmids, and pc-NF-κB plasmid (n=3). B, ChIP analysis between GSDMD and NF-κB (n=3). C, The strategy for generating mutant GSDMD promoter-driven luciferase reporters with mutated bases shown in red (n=3). D, mRNA level of *GSDMD* of adipocytes pretreated with pc-NF-κB and incubated with melatonin (MT) or not (n=6). E, LDH release was measured by ELISA of adipocytes pretreated with pc-NF-κB and incubated with melatonin (MT) or not (n=3). F, IL-1β production in the culture medium was detected by ELISA (n=3). pc-NF-κB: the overexpression plasmid of NF-κB, $GSDMD_{720}$-LUC-S1: the mutant GSDMD promoter plasmid which turns the C base to T base, $GSDMD_{720}$-LUC-S2: the mutant GSDMD promoter plasmid which turns T base to G base, $GSDMD_{720}$-LUC-S1, S2: the mutant GSDMD promoter plasmid contained two mutant sites. Values are means±SEM. **P*<.05 compared with the control group, $^{\#}P$<.05 compared with the MT group

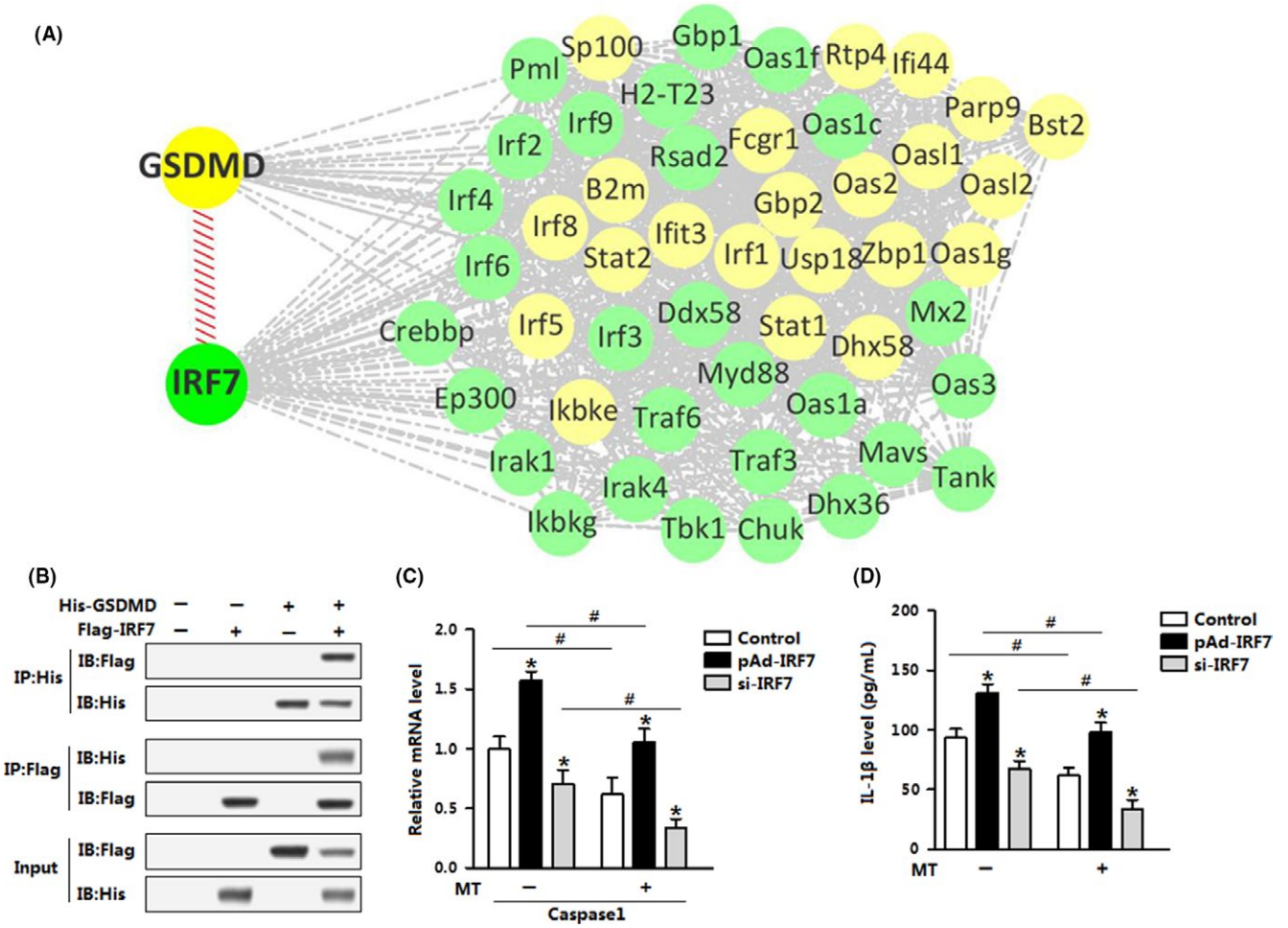

FIGURE 7 IRF7 forms a complex with GSDMD. A: Graphic representation of a network of the target genes. A, Bioinformatics analysis of the protein–protein interaction. B, GSDMD interacted with Atf4. Co-IP analysis was performed in His-GSDMD- and Flag-IRF4-transfected HEK293 cells (n=3). C, Gene expression of *Caspase1* of adipocytes infected with pAd-IRF7 or si-IRF7 and incubated with melatonin (MT) or not (n=3). D, IL-1β release in the culture medium was detected by ELISA (n=3). pAd-IRF7: overexpression adenovirus vector of IRF7. si-IRF7: interference lentivirus vector of IRF7. Values are means±SEM. **P*<.05 compared with the control group, #*P*<.05 compared with the MT group

3.8 | Melatonin reduces pyroptosis of adipose tissue in obese mice

We then studied the function of melatonin in HFD-induced pyroptosis of diet-induced obese mice. The HFD caused the pronounced increase in the mRNA and protein levels of NLRP3, ASC, IL-6, and IL-1β compared with chow diet-fed mice, whereas melatonin injection reduced these genes expressions (Figure 9A). In addition, serum IL-1β was increased in obese mice, and melatonin injection also inhibited the release of IL-1β (Figure 9B). We then measured cell death level. As expected, HFD triggered adipose pyroptosis indicated by the elevation of *Caspase1* and *GSDMD*, but did not induce adipose apoptosis, whereas melatonin decreased all these genes expressions (Figure 9C). Consistently, melatonin treatment reduced the protein levels of GSDMD and Cleaved-Caspase1 and 3 (Figure 9C). Next, we used the cotreatment of si-GSDMD and melatonin in obese mice to see whether melatonin function via GSDMD in vivo. Knockdown of GSDMD enhanced the effects of melatonin on pyroptosis (Figure 9D). And the deficiency of GSDMD significantly increased the mRNA level of *Caspase3* and the protein level of Cleaved-Caspase3, but melatonin injection had the opposite effect (Figure 9D). Together, melatonin reduced HFD-induced pyroptosis through GSDMD in obese mice adipose tissue.

4 | DISCUSSION

There exists a substantial amount of evidence supporting that melatonin exerts its anti-inflammatory effects by regulating a variety of cellular pathways.[14,17,18,39] Inflammasomes are a group of protein complexes that recognize a diverse set of inflammation-inducing stimuli and control the production of important pro-inflammatory cytokines.[21,23,40] Although studies report that melatonin inhibits the activation of inflammasome

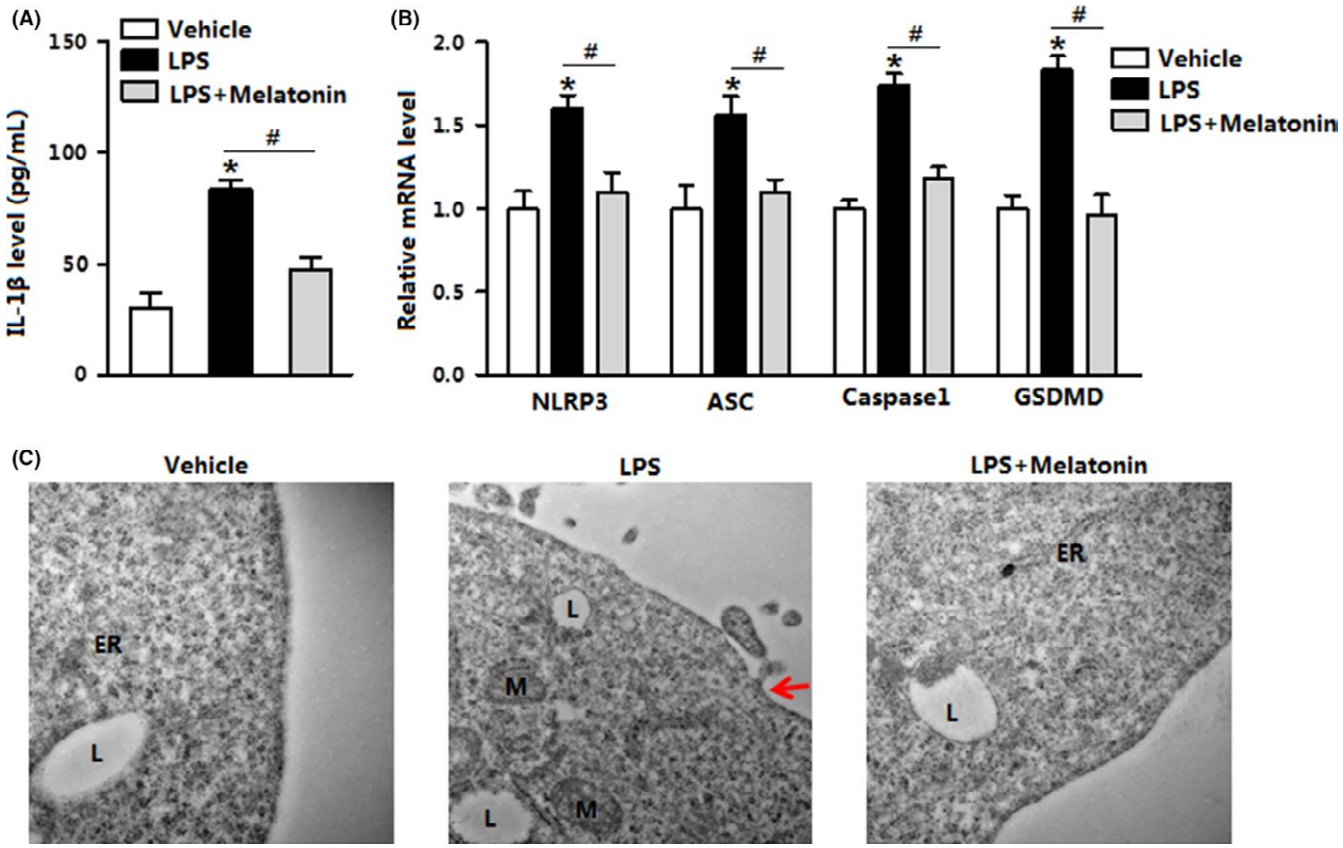

FIGURE 8 Melatonin alleviates LPS-induced pyroptosis in mice adipose tissue. Mice were injected with LPS or not and then treated with or without melatonin. A, Serum IL-1β level (n=6). B, Expression profile of *NLRP3*, *ASC*, *Caspase1*, and *GSDMD* of the mice white adipose tissue (n=6). C, Representative electron micrographs (30 000×) of treated mice adipose tissue. Red arrowhead: membrane pores, L: lipid, M: mitochondria, ER: endoplasmic reticulum (n=6). Values are means±SEM. **P*<.05 compared with the control group, $^{\#}P$<.05 compared with the LPS group

pathway in peripheral tissue such as liver and lung, the effects of melatonin on inflammasome of adipose tissue are still not determined.[28,41] In this study, we demonstrated that exogenous melatonin ameliorated inflammation of adipose tissue. Moreover, melatonin also attenuated the activation of NLRP3 inflammasome in obese or LPS-induced mice models. Thus, our data indicated that melatonin is involved in regulating inflammasome of adipocytes upon the inflammatory status.

Among the many known inflammasome complexes, the NLR pyrin domain containing 3 (NLRP3) inflammasome is best characterized and consists of NLRP3, adaptor apoptosis-associated speck-like protein (ASC), and pro-Caspase1.[42–45] There exists a substantial amount of evidence supporting that melatonin exerts its anti-inflammatory effects by inhibiting NLRP3 inflammasome.[27,46,47] To estimate the effects of melatonin on inflammasome pathway of adipocytes, we investigated the core inflammation and immune genes expression profile in adipose tissue. We found that melatonin inhibited the expression of inflammasome genes including NLRP3, ASC, Caspase1, and IL-1β. Moreover, the NF-κB signal pathway which was correlated with inflammatory response is significantly enriched by the GO analysis. Studies have identified that NF-κB could bind to TLR4 and NLRP3 promoter region, suggesting the transcriptional regulation of NF-κB on TLR4 and NLRP3 and its downstream targets.[48,49] Furthermore, melatonin could suppress NF-κB-dependent pro-inflammatory mediators in various cell types.[50–52] From these findings, we surmise that melatonin may participate in the regulation of NLRP3 inflammasome by modulating the NF-κB signal in adipocytes.

This study pointed out a significant correlation between melatonin and NF-κB signal, which had been reported.[53,54] The NF-κB signal is a cytosolic sensor which activates and promotes its nuclear translocation and DNA binding.[13,46] García et al. report that melatonin inhibits NF-κB/NLRP3 activation by regulating the nuclear RORα pathways.[55] Consistently, we demonstrated that melatonin was potent to reduce the phosphorylation of NF-κB and subsequently inhibit the NLRP3 pathway in downstream. Furthermore, melatonin also promoted the translocation of NF-κB/p65 from the nuclei to cytoplasm. These findings are consistent with other studies that NF-κB signal is central to melatonin performing the anti-inflammatory function.[53]

Inflammatory caspases cleave the gasdermin D (GSDMD) protein to trigger pyroptosis, a Caspase1-dependent form of

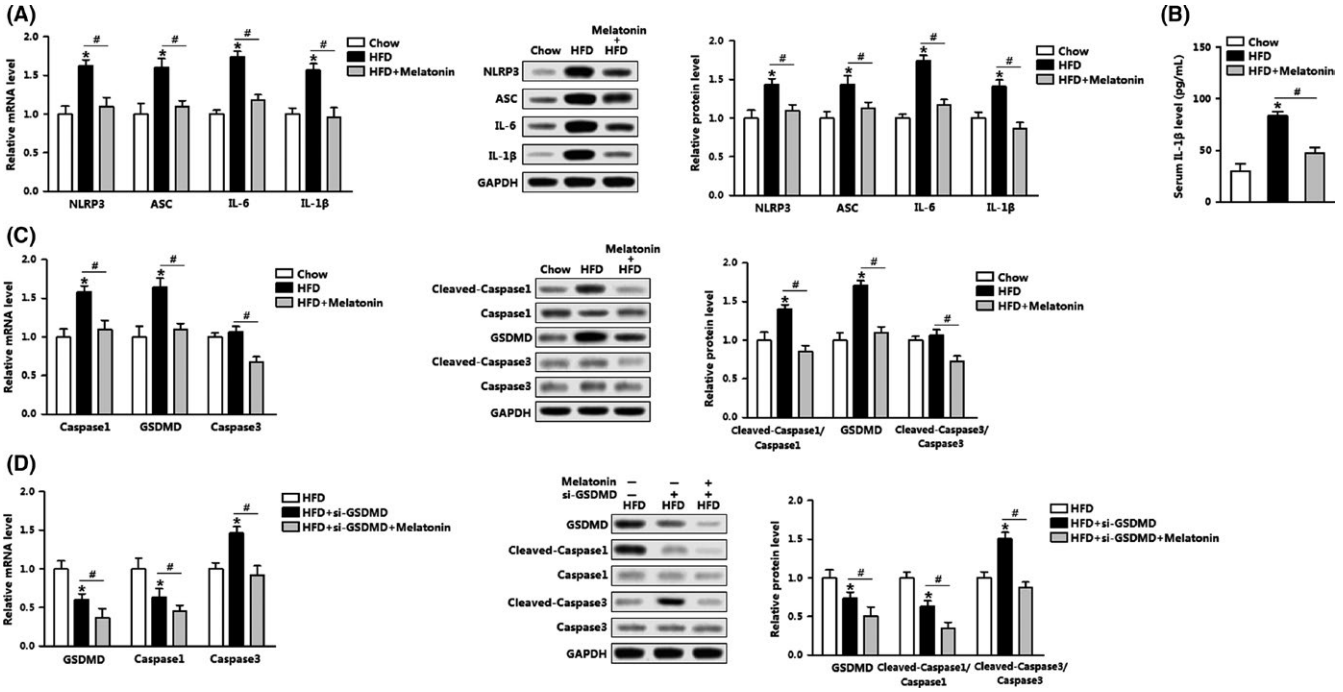

FIGURE 9 Melatonin reduces pyroptosis of adipose tissue in obese mice. A, (Left panel) Gene expression of *NLRP3*, *ASC*, *IL-6,* and *IL-1*β in the adipose tissue of high-fat-diet (HFD)-fed mice treated with melatonin or not (n=6). (Right panel) Protein levels of NLRP3, ASC, IL-6, and IL-1β in the adipose tissue of high-fat-diet (HFD)-fed mice treated with melatonin or not (n=6). B, Serum IL-1β level of high-fat-diet (HFD)-fed mice treated with melatonin or not (n=6). C, (left panel) mRNA level of *Caspase1*, *GSDMD,* and *Caspase3* in the adipose tissue of high-fat-diet (HFD)-fed mice treated with melatonin or not (n=6). (Right panel) Protein levels of Cleaved-Caspase1, Caspase1, GSDMD, Cleaved-Caspase3, and Caspase1 in the adipose tissue of high-fat-diet (HFD)-fed mice treated with melatonin or not (n=6). D, (Left panel) mRNA level of *GSDMD*, *Caspase1,* and *Caspase3* in the adipose tissue of high-fat-diet (HFD)-fed mice treated with melatonin or si-GSDMD (n=6). (Right panel) Protein levels of Cleaved-Caspase1, Caspase1, GSDMD, Cleaved-Caspase3, and Caspase1 in the adipose tissue of high-fat-diet (HFD)-fed mice treated with melatonin or si-GSDMD (n=6). si-GSDMD: interference lentivirus vector of GSDMD. Values are means±SEM. **P*<.05 compared with the control group, $^{\#}P$<.05 compared with the HFD group

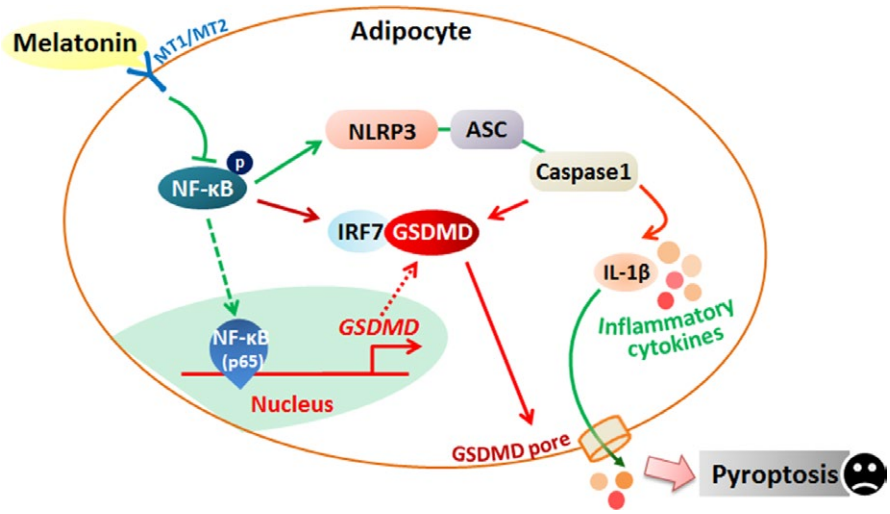

FIGURE 10 Melatonin inhibits inflammasome-induced pyroptosis through adipocytes. Melatonin blunts LPS-induced NLRP3 inflammasome activation and inhibits adipocyte pyroptosis by reducing NF-κB signal in adipocytes. IRF7 and GSDMD directly bind, and melatonin regulated GSDMD-mediated pyroptosis via the regulation of IRF7 in adipocytes. Green arrows: the classical inflammasome pathway that had been studied previously. Red arrows: the new GSDMD signal pathway that we discovered in our study

regulated cell death.[7,56,57] Pyroptosis is characterized by an early breach of the plasma membrane integrity, which results in extracellular spilling of the intracellular contents such as pro-inflammatory cytokines.[58–60] In this study, we preliminarily determined that melatonin reduced IL-1β release and attenuated pyroptosis of adipocyte. Although it is believed IL-1β production depends on the Caspase1 activity, Maelfait et al. have shown recombinant Caspase8 was able to cleave pro-IL-1β in vitro at exactly the same site as Caspase1.[61] However, our results showed melatonin reduced Caspase8 activity (Fig. S1B), and were consistent with previous studies that melatonin inhibited Caspase8 activity mainly in the cell death process.[62,63] Recent studies determine that GSDMD is the essential mediator of pyroptosis and a candidate for pyroptotic pore formation.[64,65] So we assumed that GSDMD was essential for the inhibitory role of melatonin on pyroptosis of adipocytes. In our study, we showed that melatonin decreased LPS-induced GSDMD augmentation, and along with the reduction in ASC foci formation. Notably, we are the first to demonstrate that NF-κB elevates GSDMD transcription by binding to two proximal binding sites in upstream of GSDMD promoter region. In addition, further analysis suggested that GSDMD interacted with IRF7. Although the molecular mechanism of complex formation remains elusive, we suspect that it is similar to the interaction of protein phosphatase 1 (PP1)/IRF7 by protein phosphorylation and this needs further study.[66] It is noticed that melatonin also inhibited the mRNA level of *caspase3* in adipocytes. In this study, we used Z-DVED-FMK, a specific inhibitor of Caspase3, to exclude the negative influences of apoptosis on adipocytes. However, the effects of melatonin on apoptosis of adipocyte will require further investigation. Moreover, melatonin exerts many of its physiological effects on adipose tissue not only by the action of sympathetic nervous system and its receptors in adipocyte, but also through the receptor-independent actions via its direct free radical scavenging.[67–70] Although we determined that melatonin alleviated pyroptosis by activating its receptor MT1 and MT2, the precise mechanism for inhibition of pyroptosis by melatonin needs to be further studied.

In summary, our present study demonstrates that melatonin inhibits inflammasome-induced pyroptosis of adipocytes. Moreover, NF-κB/GSDMD signal is essential for melatonin inhibiting NLRP3 inflammasome formation and inflammatory cytokines release in adipocytes pyroptosis (Figure 10). Thus, our results indicate that melatonin has potential as anti-obesity agent to reverse obesity-related systemic inflammation.

ACKNOWLEDGEMENTS

This work was supported by the grants from the Major National Scientific Research Projects (2015CB943102) and the National Nature Science Foundation of China (31572365).

CONFLICT OF INTEREST

The authors declare that there is no duality of interest associated with this manuscript.

AUTHOR CONTRIBUTIONS

All the authors contributed to this manuscript. Z.L., L.G., and C.S. planned for experiments; all the authors performed experiments; Z.L., Y.X. and D.L. analyzed data; Q.R., S.W., and Y.X. contributed reagents or other essential materials; L.G. and Z.L. wrote the paper.

REFERENCES

1. Lumeng CN, Saltiel AR. Inflammatory links between obesity and metabolic disease. *J Clin Invest*. 2011;121:2111-2117.
2. Szewczyk-golec K, Wozniak A, Reiter RJ. Inter-relationships of the chronobiotic, melatonin, with leptin and adiponectin: implications for obesity. *J Pineal Res*. 2015;59:277-2791.
3. Zhang LJ, Guerrero-juarez CF, Hata T, et al. Innate immunity. Dermal adipocytes protect against invasive Staphylococcus aureus skin infection. *Science*. 2015;347:67-71.
4. Henao-mejia J, Elinav E, Jin C, et al. Inflammasome-mediated dysbiosis regulates progression of NAFLD and obesity. *Nature*. 2012;482:179-185.
5. Gurung P, Lukens JR, Kanneganti TD. Mitochondria: diversity in the regulation of the NLRP3 inflammasome. *Trends Mol Med*. 2015;21:193-201.
6. Shi J, Gao W, Shao F. Pyroptosis: Gasdermin-Mediated Programmed Necrotic Cell Death. *Trends Biochem Sci*. 2017;42:245-254.
7. Vande Walle L, Lamkanfi M. Pyroptosis. *Curr Biol* 2016;26:R568-R572.
8. Hardeland R, Madrid JA, Tan DX, et al. Melatonin, the circadian multioscillator system and health: the need for detailed analyses of peripheral melatonin signaling. *J Pineal Res*. 2012;52:139-166.
9. De Farias Tda S, De Oliveira AC, Andreotti S, et al. Pinealectomy interferes with the circadian clock genes expression in white adipose tissue. *J Pineal Res*. 2015;58:251-261.
10. Reiter RJ. Pineal melatonin: cell biology of its synthesis and of its physiological interactions. *Endocr Rev*. 1991;12:151-180.
11. Kedziora-Kornatowska K, Szewczyk-Golec K, Czuczejko J, et al. Effect of melatonin on the oxidative stress in erythrocytes of healthy young and elderly subjects. *J Pineal Res*. 2007;42:153-158.
12. Kedziora-Kornatowska K, Szewczyk-Golec K, Kozakiewicz M, et al. Melatonin improves oxidative stress parameters measured in the blood of elderly type 2 diabetic patients. *J Pineal Res*. 2009;46:333-337.
13. Manchester LC, Coto-montes A, Boga JA, et al. Melatonin: an ancient molecule that makes oxygen metabolically tolerable. *J Pineal Res*. 2015;59:403-419.
14. Mauriz JL, Collado PS, Veneroso C, et al. A review of the molecular aspects of melatonin's anti-inflammatory actions: recent insights and new perspectives. *J Pineal Res*. 2013;54:1-14.
15. Liu Z, Gan L, Luo D, et al. Melatonin promotes circadian rhythm-induced proliferation through Clock/histone deacetylase 3/c-Myc

interaction in mouse adipose tissue in mice adipose tissue. *J Pineal Res* 2017;62:e12383.
16. Chen J, Qian C, Duan H, et al. Melatonin attenuates neurogenic pulmonary edema via the regulation of inflammation and apoptosis after subarachnoid hemorrhage in rats. *J Pineal Res*. 2015;59:469-477.
17. Cano Barquilla P, Pagano ES, Jimenez-ortega V, et al. Melatonin normalizes clinical and biochemical parameters of mild inflammation in diet-induced metabolic syndrome in rats. *J Pineal Res* 2014;57:280-290.
18. Muxel SM, Laranjeira-silva MF, Carvalho-sousa CE, et al. The RelA/cRel nuclear factor-kappaB (NF-kappaB) dimer, crucial for inflammation resolution, mediates the transcription of the key enzyme in melatonin synthesis in RAW 264.7 macrophages. *J Pineal Res*. 2016;60:394-404.
19. Zhao L, An R, Yang Y, et al. Melatonin alleviates brain injury in mice subjected to cecal ligation and puncture via attenuating inflammation, apoptosis, and oxidative stress: the role of SIRT1 signaling. *J Pineal Res*. 2015;59:230-239.
20. Carrillo-vico A, Lardone PJ, Naji L, et al. Beneficial pleiotropic actions of melatonin in an experimental model of septic shock in mice: regulation of pro-/anti-inflammatory cytokine network, protection against oxidative damage and anti-apoptotic effects. *J Pineal Res*. 2005;39:400-408.
21. Strowig T, Henao-mejia J, Elinav E, et al. Inflammasomes in health and disease. *Nature*. 2012;481:278-286.
22. Liston A, Masters SL. Homeostasis-altering molecular processes as mechanisms of inflammasome activation. *Nat Rev Immunol*. 2017;17:208-214.
23. Schroder K, Tschopp J. The inflammasomes. *Cell*. 2010; 140:821-832.
24. Horng T, Hotamisligil GS. Linking the inflammasome to obesity-related disease. *Nat Med*. 2011;17:164-165.
25. Henao-mejia J, Elinav E, Thaiss CA, et al. Inflammasomes and metabolic disease. *Annu Rev Physiol*. 2014;76:57-78.
26. Murphy AJ, Kraakman MJ, Kammoun HL, et al. IL-18 Production from the NLRP1 Inflammasome Prevents Obesity and Metabolic Syndrome. *Cell Metab*. 2016;23:155-164.
27. Dong Y, Fan C, Hu W, et al. Melatonin attenuated early brain injury induced by subarachnoid hemorrhage via regulating NLRP3 inflammasome and apoptosis signaling. *J Pineal Res*. 2016;60:253-262.
28. Zhang Y, Li X, Grailer JJ, et al. Melatonin alleviates acute lung injury through inhibiting the NLRP3 inflammasome. *J Pineal Res*. 2016;60:405-414.
29. Aglietti RA, Estevez A, Gupta A, et al. GsdmD p30 elicited by caspase-11 during pyroptosis forms pores in membranes. *Proc Natl Acad Sci USA*. 2016;113:7858-7863.
30. Bergsbaken T, Fink SL, Cookson BT. Pyroptosis: host cell death and inflammation. *Nat Rev Microbiol*. 2009;7:99-109.
31. Howrylak JA, Nakahira K. Inflammasomes: Key Mediators of Lung Immunity. *Annu Rev Physiol*. 2017;79:471-494.
32. Li R, Zhang LM, Sun WB. Erythropoietin rescues primary rat cortical neurons from pyroptosis and apoptosis via Erk1/2-Nrf2/Bach1 signal pathway. *Brain Res Bull*. 2017;130:236-244.
33. Jorgensen I, Rayamajhi M, Miao EA. Programmed cell death as a defence against infection. *Nat Rev Immunol*. 2017;17:151-164.
34. Giordano A, Murano I, Mondini E, et al. Obese adipocytes show ultrastructural features of stressed cells and die of pyroptosis. *J Lipid Res*. 2013;54:2423-2436.
35. Gan L, Liu Z, Cao W, et al. FABP4 reversed the regulation of leptin on mitochondrial fatty acid oxidation in mice adipocytes. *Sci Rep*. 2015;5:13588.
36. Zhong Z, Umemura A, Sanchez-lopez E, et al. NF-kappaB Restricts Inflammasome Activation via Elimination of Damaged Mitochondria. *Cell*. 2016;164:896-910.
37. Liu Z, Gan L, Wu T, et al. Adiponectin reduces ER stress-induced apoptosis through PPARalpha transcriptional regulation of ATF2 in mouse adipose. *Cell Death Dis*. 2016;7:e2487.
38. Gan L, Liu Z, Wu T, et al. alphaMSH promotes preadipocyte proliferation by alleviating ER stress-induced leptin resistance and by activating Notch1 signal in mice. *Biochim Biophys Acta*. 2016;1863:231-238.
39. Agil A, Reiter RJ, Jimenez-aranda A, et al. Melatonin ameliorates low-grade inflammation and oxidative stress in young Zucker diabetic fatty rats. *J Pineal Res*. 2013;54:381-388.
40. Davis BK, Wen H, Ting JP. The inflammasome NLRs in immunity, inflammation, and associated diseases. *Annu Rev Immunol*. 2011;29:707-735.
41. Cao Z, Fang Y, Lu Y, et al. Melatonin alleviates cadmium-induced liver injury by inhibiting the TXNIP-NLRP3 inflammasome. *J Pineal Res*. 2017;62:e12389.
42. Gross CJ, Gross O. PKA Has the Gall to Oppose NLRP3. *Immunity*. 2016;45:707-709.
43. Leavy O. Inflammasome: Turning on and off NLRP3. *Nat Rev Immunol*. 2013;13:1.
44. Tschopp J, Schroder K. NLRP3 inflammasome activation: the convergence of multiple signalling pathways on ROS production? *Nat Rev Immunol*. 2010;10:210-215.
45. Miao EA, Leaf IA, Treuting PM, et al. Caspase-1-induced pyroptosis is an innate immune effector mechanism against intracellular bacteria. *Nat Immunol*. 2010;11:1136-1142.
46. Volt H, Garcia JA, Doerrier C, et al. Same molecule but different expression: aging and sepsis trigger NLRP3 inflammasome activation, a target of melatonin. *J Pineal Res*. 2016;60:193-205.
47. Ortiz F, Acuna-castroviejo D, Doerrier C, et al. Melatonin blunts the mitochondrial/NLRP3 connection and protects against radiation-induced oral mucositis. *J Pineal Res*. 2015;58:34-49.
48. Bonin CP, Baccarin RY, Nostell K, et al. Lipopolysaccharide-induced inhibition of transcription of tlr4 in vitro is reversed by dexamethasone and correlates with presence of conserved NFkappaB binding sites. *Biochem Biophys Res Commun*. 2013;432:256-261.
49. Qiao Y, Wang P, Qi J, et al. TLR-induced NF-kappaB activation regulates NLRP3 expression in murine macrophages. *FEBS Lett*. 2012;586:1022-1026.
50. Shiu SY, Leung WY, Tam CW, et al. Melatonin MT1 receptor-induced transcriptional up-regulation of p27 (Kip1) in prostate cancer antiproliferation is mediated via inhibition of constitutively active nuclear factor kappa B (NF-kappaB): potential implications on prostate cancer chemoprevention and therapy. *J Pineal Res*. 2013;54:69-79.
51. Lin YW, Lee LM, Lee WJ, et al. Melatonin inhibits MMP-9 transactivation and renal cell carcinoma metastasis by suppressing Akt-MAPKs pathway and NF-kappaB DNA-binding activity. *J Pineal Res*. 2016;60:277-290.
52. Rahim I, Djerdjouri B, Sayed RK, et al. Melatonin administration to wild-type mice and non-treated NLRP3 mutant mice share

similar inhibition of the inflammatory response during sepsis. *J Pineal Res* 2017;62:e12410.

53. Gao Y, Xiao X, Zhang C, et al. Melatonin synergizes the chemotherapeutic effect of 5-fluorouracil in colon cancer by suppressing PI3K/AKT and NF-kappaB/iNOS signaling pathways. *J Pineal Res*. 2017;62:e12380.
54. Ren W, Liu G, Chen S, et al. Melatonin signaling in T cells: functions and applications. *J Pineal Res* 2017;62:e12394.
55. Garcia JA, Volt H, Venegas C, et al. Disruption of the NF-kappaB/NLRP3 connection by melatonin requires retinoid-related orphan receptor-alpha and blocks the septic response in mice. *FASEB J*. 2015;29:3863-3875.
56. Ding J, Wang K, Liu W, et al. Pore-forming activity and structural autoinhibition of the gasdermin family. *Nature*. 2016;535:111-116.
57. Jorgensen I, Miao EA. Pyroptotic cell death defends against intracellular pathogens. *Immunol Rev*. 2015;265:130-142.
58. Lamkanfi M, Dixit VM. Inflammasomes and their roles in health and disease. *Annu Rev Cell Dev Biol*. 2012;28:137-161.
59. Fink SL, Cookson BT. Apoptosis, pyroptosis, and necrosis: mechanistic description of dead and dying eukaryotic cells. *Infect Immun*. 2005;73:1907-1916.
60. Kayagaki N, Stowe IB, Lee BL, et al. Caspase-11 cleaves gasdermin D for non-canonical inflammasome signalling. *Nature*. 2015;526:666-671.
61. Maelfait J, Vercammen E, Janssens S, et al. Stimulation of Toll-like receptor 3 and 4 induces interleukin-1beta maturation by caspase-8. *J Exp Med*. 2008;205:1967-1973.
62. Das A, Mcdowell M, Pava MJ, et al. The inhibition of apoptosis by melatonin in VSC4.1 motoneurons exposed to oxidative stress, glutamate excitotoxicity, or TNF-alpha toxicity involves membrane melatonin receptors. *J Pineal Res* 2010;48:157-169.
63. Espino J, Rodriguez AB, Pariente JA. The inhibition of TNF-alpha-induced leucocyte apoptosis by melatonin involves membrane receptor MT1/MT2 interaction. *J Pineal Res*. 2013;54:442-452.
64. Sborgi L, Ruhl S, Mulvihill E, et al. GSDMD membrane pore formation constitutes the mechanism of pyroptotic cell death. *EMBO J*. 2016;35:1766-1778.
65. Shi J, Zhao Y, Wang K, et al. Cleavage of GSDMD by inflammatory caspases determines pyroptotic cell death. *Nature*. 2015;526:660-665.
66. Wang L, Zhao J, Ren J, et al. Protein phosphatase 1 abrogates IRF7-mediated type I IFN response in antiviral immunity. *Eur J Immunol*. 2016;46:2409-2419.
67. Galano A, Tan DX, Reiter RJ. Melatonin as a natural ally against oxidative stress: a physicochemical examination. *J Pineal Res*. 2011;51:1-16.
68. Galano A, Medina ME, Tan DX, et al. Melatonin and its metabolites as copper chelating agents and their role in inhibiting oxidative stress: a physicochemical analysis. *J Pineal Res*. 2015;58:107-116.
69. Alonso-vale MI, Peres SB, Vernochet C, et al. Adipocyte differentiation is inhibited by melatonin through the regulation of C/EBPbeta transcriptional activity. *J Pineal Res*. 2009;47:221-227.
70. Wu SM, Lin WY, Shen CC, et al. Melatonin set out to ER stress signaling thwarts epithelial mesenchymal transition and peritoneal dissemination via calpain-mediated C/EBPbeta and NFkappaB cleavage. *J Pineal Res*. 2016;60:142-154.

SUPPORTING INFORMATION

Additional Supporting Information may be found online in the supporting information tab for this article.

How to cite this article: Liu Z, Gan L, Xu Y, et al. Melatonin alleviates inflammasome-induced pyroptosis through inhibiting NF-κB/GSDMD signal in mice adipose tissue. *J Pineal Res*. 2017;63:e12414. https://doi.org/10.1111/jpi.12414